Published June 7, 2021, doi:10.4049/jimmunol.2000768



# Spacer Length Modification Facilitates Discrimination between Normal and Neoplastic Cells and Provides Clinically Relevant CD37 CAR T Cells

**Shingo Okuno*,[1] Yoshitaka Adachi,*,[1] Seitaro Terakura,* Jakrawadee Julamanee,*,† Toshiyasu Sakai,* Koji Umemura,* Kotaro Miyao,* Tatsunori Goto,* Atsushi Murase,* Kazuyuki Shimada,* Tetsuya Nishida,* Makoto Murata,* and Hitoshi Kiyoi***

**Despite the remarkable initial efficacy of CD19 chimeric Ag receptor T (CAR-T) cell therapy, a high incidence of relapse has been observed. To further increase treatment efficacy and reduce the rate of escape of Ag-negative cells, we need to develop CAR-T cells that target other Ags. Given its restricted expression pattern, CD37 was considered a preferred novel target for immunotherapy in hematopoietic malignancies. Therefore, we designed a CD37-targeting CAR-T (CD37CAR-T) using the single-chain variable fragment of a humanized anti-CD37 Ab, transmembrane and intracellular domains of CD28, and CD3ζ signaling domains. High levels of CD37 expression were confirmed in B cells from human peripheral blood and bone marrow B cell precursors at late developmental stages; by contrast, more limited expression of CD37 was observed in early precursor B cells. Furthermore, we found that human CD37CAR-T cells with longer spacer lengths exhibited high gene transduction efficacy but reduced capacity to proliferate; this may be due to overactivation and fratricide. Spacer length optimization resulted in a modest transduction efficiency together with robust capacity to proliferate. CD37CAR-T cells with optimized spacer length efficiently targeted various CD37$^+$ human tumor cell lines but had no impact on normal leukocytes both in vitro and in vivo. CD37CAR-T cells effectively eradicated Raji cells in xenograft model. Collectively, these results suggested that spacer-optimized CD37CAR-T cells could target CD37-high neoplastic B cells both in vitro and in vivo, with only limited interactions with their normal leukocyte lineages, thereby providing an additional promising therapeutic intervention for patients with B cell malignancies.** ***The Journal of Immunology*****, 2021, 206: 1–13.**

Several modes of cancer immunotherapy, including native or drug-conjugated antitumor Abs, immune checkpoint inhibitors, and chimeric Ag receptor T (CAR-T) cells have been administered in patients in clinical settings and have resulted notably improved outcomes (1–7). Among these novel therapeutic options, administration of CD19-targeting CAR-T (CD19CAR-T) has dramatically improved the complete remission rate for B cell acute lymphoblastic leukemia (B-ALL) and diffuse large B cell lymphoma (DLBCL); CD19CAR-T therapy has recently been approved for relapsed/refractory B-ALL and DLBCL (8–10). However, relapses were observed even among B-ALL patients who achieved complete remission in response to CD19CAR-T cell therapy, and only ∼40% of patients achieved long-term survival (11). Furthermore, approximately one third of relapses were CD19 negative (3, 12, 13), and the efficacy of CD19CAR-T therapy for the treatment of DLBCL is slightly inferior to the responses seen in B-ALL. As such, new therapies targeting other Ags are needed to improve overall therapeutic efficacy and to prevent immunological escape secondary to CD19 Ag loss.

CD37 is a four–transmembrane (TM) protein and belongs to the tetraspanin superfamily. The molecular function of tetraspanins as a group has not been completely elucidated. All immune cells express one or more tetraspanins of various types (14). The tetraspanin CD37 promotes survival of IgG1-producing B cells via α4β1 integrin signals (15) and negatively regulates TCR signaling (16) and peptide/MHC presentation from APCs (17). Previous reports have documented that CD37 expression is restricted to immune cells; it is highly expressed in mature B cells (14, 16, 18, 19) and to a limited extent in immune cells other than B cells (20). High levels of CD37 were detected in mature B cell tumors including follicular lymphoma,

*Department of Hematology and Oncology, Nagoya University Graduate School of Medicine, Nagoya, Japan; and †Division of Clinical Hematology, Faculty of Medicine, Prince of Songkla University, Songkhla, Thailand

[1]S.O. and Y.A. equally contributed to this work.

ORCIDs: 0000-0002-7477-0986 (S.O.); 0000-0002-9763-5533 (Y.A.); 0000-0002-1194-8046 (S.T.); 0000-0002-6526-9479 (J.J.); 0000-0002-3530-7817 (T.S.); 0000-0003-3459-0478 (K.U.); 0000-0003-0716-1424 (K.M.); 0000-0002-0314-9498 (T.G.); 0000-0002-1075-9219 (K.S.); 0000-0001-6382-9498 (H.K.).

Received for publication June 30, 2020. Accepted for publication April 14, 2021.

This work was supported by Japan Society for the Promotion of Science KAKENHI Grants 15k09497 and 18k08351 (to S.T.), Practical Research for Innovative Cancer Control Grants 15ck0106067h0002 and 17ck0106291h0001 (to S.T.), and Practical Research Project for Allergic Diseases and Immunology 19ek0510022h0003 (to S.T. and M.M.). J.J. was supported by Research Foundation of Prince of Songkla University Grant MOE. 0521.1.0601(2)/6058.

Conception and design: S.O. and S.T. Development of methodology: S.O. and S.T. Acquisition of data: S.O., Y.A., S.T., J.J., T.S., K.U., K.M., T.G., and T.N. Sample collection: A.M. and K.S. Analysis and interpretation of data: S.O., Y.A., and S.T. Writing, review, and/or revision of the manuscript: S.O., S.T., M.M., and H.K. Study supervision: S.T., M.M., and H.K.

Address correspondence and reprint requests to Dr. Seitaro Terakura, Department of Hematology and Oncology, Nagoya University Graduate School of Medicine, 65 Tsurumai-cho, Showa-ku, Nagoya, Aichi 466-8560, Japan. E-mail address: tseit@med.nagoya-u.ac.jp

The online version of this article contains supplemental material.

Abbreviations used in this article: 7AAD, 7-aminoactinomycin D; ABC, Ab-binding capacity; B-ALL, B cell acute lymphoblastic leukemia; BM, bone marrow; CAR-T, chimeric Ag receptor T; CD19CAR-T, CD19-targeting CAR-T; CD37CAR-T, CD37-targeting CAR-T; CD37$^+$K562, CD37-positive K562; CTV, CellTrace Violet; DLBCL, diffuse large B cell lymphoma; hCD, human CD; MFI, mean fluorescence intensity; NOG, NOD/Shi-scid IL-2Rγ knockout; PB, peripheral blood; PI, propidium iodide; Raji-ffluc, Raji cell expressing firefly luciferase; sABC, specific ABC; scFv, single-chain variable fragment; St, streptavidin; tEGFR, truncated version of the epidermal growth factor receptor; TM, transmembrane.

mantle cell lymphoma, and chronic lymphocytic leukemia (21–23) and in some T cell tumors (24). By contrast, CD37 expression was not detected in B-ALL or multiple myeloma (21). As such, CD37 may be an ideal target for new immunotherapeutic strategies because of its restricted expression pattern among normal leukocytes and robust expression in association with specific neoplastic diseases (25, 26). Because CD37 is considered to be one of the most promising targets for the development of new immunotherapies, we have focused our studies on CAR-T cell therapy that targets this Ag.

CAR-T cell therapy is a revolutionary and effective treatment option for various tumors; the chimeric receptors facilitate recognition of specific targets and may continue to function until the Ag-positive cells are fully eradicated. Interestingly, there are reports of profound B cell deficiency developing in response to CD19CAR-T cell therapy (27–29); this relatively common event was not fatal and could be ameliorated with i.v. Ig. By contrast, complete eradication of T cells, neutrophils, and monocytes will likely result in a more fatal immunodeficiency (30). As such, evaluation of CD37 expression together with optimization of the affinity for CD37 are important features of any new CD37-targeting CAR-T (CD37CAR-T) cells. Numerous factors contribute to the comparative affinity and cytotoxic activity of CAR molecules, most notably the precise nature of the hypervariable region that directly recognizes CD37; however, the nature and length of the spacer domain that connects the hypervariable and TM region may also have an impact on the overall outcome (31–34). Two previous reports demonstrated the development of CD37CAR-T, in which they did not mention any significant fratricide of the CD37CAR-T cells (35, 36). We observed growth inhibition during culture in CD37CAR-T with longer spacer domain. Thereafter, we developed a novel, to our knowledge, CD37CAR molecule with optimized spacer length that retains excellent antitumor efficacy with minimal impact on normal $CD37^+$ cells.

## Materials and Methods

### *Cell lines*

The Karpas1106P tumor cell line was obtained from the European Collection of Authenticated Cell Cultures. The SUP-T1 and MM1-S tumor cell lines were obtained from the American Type Culture Collection. Tumor cell lines including K562, Daudi, Raji, NAB, ALL-1, B-ALL-1, Ramos, SU-DHL4, SU-DHL6, SU-DHL10, Molt-4, NPhA1, Kasumi-1, MV4-11, OCI-AML3, MOLM-13, HL-60, NOMO-1, OCI–Ly-1, OCI–Ly-10, U266, Jurkat, Will-2, NALM-6, and ATN-1 were maintained in our laboratory. Dr. N. Hosen (Osaka University, Osaka, Japan) kindly provided us with the KMS-12-BM, RPMI 8226, and NCI-H929 tumor cell lines. To create CD37-positive K562 ($CD37^+$K562) cells, we cloned full-length CD37 cDNA from Ramos cells and transduced K562 cells via a retroviral vector described elsewhere (37). Raji cells expressing firefly luciferase (Raji-ffluc) were generated by lentiviral transduction with the GFP-ffluc gene, followed by FACS for GFP expression.

### *Human subjects*

The research protocols of this study were approved by the Institutional Review Board of Nagoya University Graduate School of Medicine (approval number 2014-0081). Peripheral blood (PB) cells, bone marrow (BM) cells, and tumor cells were obtained from patients or healthy donors after written informed consent was obtained in accordance with the Declaration of Helsinki.

### *Quantification of CD37 molecules*

CD37 expression on the surface of PB cells from healthy donors was evaluated using QIFIKIT (Dako, Glostrup, Denmark) described elsewhere (37). Ab-binding capacity (ABC; molecules per cell) was determined on the basis of the results from a standard regression line between fluorescence intensity and Ag density. Specific ABC (sABC) was determined by subtracting the background Ab equivalents from the isotype control (38).

### *Anti-CD37CAR design and vector construction*

To generate CD37CAR constructs, we created single-chain variable fragments (scFv) based on sequences from an anti-CD37 Ab (CD37 scFv sequence; Supplemental Table I). The CD37CAR construct also included the hinge, the CD28 TM domain, the CD28 intracellular domain, and the CD3ζ signaling domain. CD37CAR was fused to a truncated version of the epidermal growth factor receptor (tEGFR) that lacked the epidermal growth factor binding and intracellular signaling domains located downstream of the self-cleaving T2A sequence (39, 40). Cell surface tEGFR was detected using the biotinylated Erbitux (cetuximab) mAb for EGFR (Bristol-Myers Squibb, New York, NY). In the previous reports, we have shown that the CAR staining and tEGFR staining can demonstrate transduction efficiency with comparable results and high reproducibility (37, 40). The CD37CAR transgenes were assembled and packaged into LZRS–pBMN-Z by NEBuilder HiFi DNA Assembly Cloning Kit (New England BioLabs, Ipswich, MA). CD37CAR-encoding retrovirus was produced using the Phoenix-Ampho system (Orbigen, San Diego, CA).

### *Generation, expansion, and selection of CD37CAR-transduced, CD8-positive T cells*

Except where indicated, all CAR-transduced cells were generated from $CD8^+$ T cells. $CD8^+$ T cells were purified with anti-CD8 immunomagnetic beads (Miltenyi Biotec, Bergisch Gladbach, Germany) from healthy donor PBMCs; these cells were activated with anti-CD3/CD28 beads (Invitrogen, Carlsbad, CA) and cultured in RPMI 1640 medium containing 10% human serum, 0.8 mM L-glutamine, 1% penicillin–streptomycin, 0.5 μM 2-ME, and recombinant human IL-2 to a final concentration of 50 IU/ml. On days 3 and 4 of culture, activated $CD8^+$ T cells were transduced by centrifugation at 2100 rpm for 120 min at 32°C on recombinant human fibronectin (RetroNectin; Takara Bio, Otsu, Japan) preloaded with the retroviral vector. At 3 d after transduction, CD37CAR-tEGFR–positive cells were selected by the biotinylated Erbitux Ab and anti-biotin immunomagnetic beads (Miltenyi Biotec). Purified CD37CAR-T cells were restimulated with anti-CD3/CD28 beads and expanded for subsequent experiments.

### *Flow cytometry*

All samples were analyzed by flow cytometry on the FACSAria II and FACSCanto II (BD Biosciences, San Jose, CA) and analyzed with FlowJo (Tree Star, Ashland, OR).

### *Ab information*

Biotinylated Erbitux and streptavidin (St)–PE or St-BV421 were used to identify cells that expressed tEGFR. All fluorescent dye–conjugated Abs were from the manufacturers indicated: St-PE, St-APC, and St-BV421, CD8-APC (clone RPA-T8), CD10-PE (HI10α), CD19–PE-Cy7 (HIB19), IFN-γ–FITC (4S.B3), IL-2–APC (5344.111), and CD45RA-FITC (L48) were from BD Biosciences and purified unconjugated anti-CD37 and CD37-FITC (M-B371) were from BioLegend (San Diego, CA). Reagents used in the humanized mice experiments including anti–human CD (hCD)45–APC (HI30), anti-hCD3–APC-Cy7 (UCHT1), anti-hCD33–APC (WM53), anti-hCD34–PE (581), anti-mouse CD45-PerCP (30-F11), and 2-(4-amidinophenyl)-1H-indole-6-carboxamidine solution were obtained from BD Biosciences. Anti-hCD45–APC–Alexa Fluor 750 (HI30) was obtained from Thermo Fisher Scientific (Waltham, MA). Before using PB or BM samples for flow cytometry, RBCs were lysed using BD FACS Lysing Solution (BD Biosciences).

### *Annexin V/propidium iodide assay*

CD37-negative cell line NALM6 was lentivirally transduced with CD37, and $CD37^+$NALM6 was sorted into untransduced, low (CD37-low), middle (CD37-middle), and high (CD37-high) NALM6 by CD37 expression levels. To identify apoptotic cells derived from CAR-T cells and NALM6 differentially, CD37CAR-T cells were stained by CellTrace Violet (CTV; Thermo Fisher Scientific). CD37CAR-T cells were cocultured in a 1:1 mixture with NALM6 cell lines and then stained using APC annexin V apoptosis detection kit with propidium iodide (PI) (BioLegend) according to the manufacturer's protocol at 4, 8, and 24 h poststimulation.

### *Fratricide analysis*

$CD3^+$ T cells were isolated with anti-CD3 immunomagnetic beads (Miltenyi Biotec) from donor PBMCs and were separately cultured as target cells and CD37CAR-T cells. The CD37CAR-T cells with various spacer lengths and tEGFR-T cells were generated as described in the previous paragraph. The autologous target cells were stimulated with CD3/28 beads and IL-2 50 U/ml every 3 d for 10 d. On day 10, the target cells were stained by CTV and cocultured in a 1:1 mixture with autologous CD37CAR-T cells with IL-2 20

U/ml. After 24 h of coculture, cells were analyzed by flow cytometry. For live cell enumeration, 7-aminoactinomycin D (7AAD)–negative live cells were first gated, then the percentages of $CTV^-$ and $CTV^+$ cells were calculated. For annexin V/PI analysis, all $CTV^+$ target cells were gated, then annexin $V^+$ apoptotic cells were enumerated within $CTV^+$ target cell gate.

### *Intracellular phospho-flow analysis*

CAR-T cells and Raji tumor cells ($CD19^+$ and $CD37^+$) were mixed at a 1:5 ratio, spun down briefly, and incubated at 37°C for 5 min for phospho-CD3ζ and for 30 min for phospho-p38 and phospho-ERK. Cells were then fixed by the addition of 2% paraformaldehyde at 37°C for 10 min, permeabilized in ice-cold 90% methanol, and left on ice for 30 min. For staining, the following phospho-specific Abs were used: CD3ζ (pY142, clone K25-407.69; PE-conjugated; BD Biosciences), p38 (pT180/pY182, clone D3F9; unconjugated; Cell Signaling Technology, Danvers, MA), and ERK1/2 (pT202/pY204; unconjugated; Cell Signaling Technology) and donkey anti-rabbit IgG–Alexa Fluor 647 (secondary Ab; BioLegend).

### *Intracellular cytokine staining*

CD37CAR-T cells and CD37-K562 were mixed at a 1:1 ratio in the presence of brefeldin A (Sigma-Aldrich) and then fixed and permeabilized with Cell Fixation/Permeabilization Kits (BD Biosciences) for evaluation of intracellular cytokine expression. After fixation, CTLs were identified with anti-CD8 mAb. The presence of intracellular anti–IFN-γ and anti–IL-2 were detected using specific Abs noted earlier (BD Biosciences). In experiments with patient-derived tumor cells, cells from thawed samples were applied to a Dead Cell Removal Kit (Miltenyi Biotec) to purify live cells according to the manufacturer's instructions.

### *Raji tumor cell xenograft model*

The murine experimental procedures were approved by the Institutional Animal Care and Use Committee of Nagoya University Graduate School of Medicine (approval number: 20266). Seven-week-old male NOD/Shi-scid IL-2Rγ knockout (NOG) mice were inoculated with $5 \times 10^5$ Raji-ffluc cells via tail vein injection. Seven days later, $5 \times 10^6$ $tEGFR^+$ T cells, CD37CAR-T cells, or CD19CAR-T cells were transferred to the mice also by tail vein i.v. injection. For bioluminescence-based measurement of tumor growth, animals were injected i.p. with 10 μl/g body weight of 15 mg/ml firefly D-luciferin in PBS. Tumor progression was monitored every 7 d with the IVIS Spectrum System (Caliper Life Science, Waltham, MA).

### *Generation of the humanized mice model*

$hCD34^+$ cells were isolated from cord blood obtained from Chubu Cord Blood Bank (Seto, Japan) using immunomagnetic beads (EasySep Human CD34 Positive Kit II; VERITAS, Santa Clara, CA). The isolated $CD34^+$ cells were stored in liquid nitrogen until use. Seven-week-old male NOG mice were sublethally irradiated with 1.5 Gy (Hitachi Medical Corporation, Tokyo, Japan). On the following day, mice were inoculated with $3.6 \times 10^4$ $hCD34^+$ cells by i.v. injection. Twelve weeks later, BM aspiration was performed from the femurs of these mice, and engraftment of $hCD45^+$ cells was confirmed (41). The following day, these mice received $5 \times 10^6$ control T cells, CD37CAR-T cells, or CD19CAR-T cells by i.v. injection. Seven days later, the mice were sacrificed, and BM was collected from both femurs, and the frequencies of hCD45, hCD3, hCD33, hCD34, hCD19, and hCD37 were assessed by flow cytometry.

### *Statistical analysis*

All experimental data are presented as mean ± SEM. Data were analyzed using paired two-tailed Student *t* tests to evaluate statistical differences between two groups. Differences among three or more groups were evaluated with one-way ANOVA, followed by Bonferroni test. Two-way ANOVA followed by Bonferroni multiple comparison test was used to assess differences among multiple treatment groups. Statistical analysis was performed on GraphPad Prism 8 software (GraphPad Software, La Jolla, CA).

## Results

### *CD37 expression in normal BM and PB leukocytes and in activated T cells*

CD37 expression has been reported to be high in some lymphoid cells and weak in cells from other leukocyte lineages (21, 42). To confirm the tissue restriction of CD37, we explored its expression by PB leukocytes from healthy donors (Fig. 1A). Some of the cells within the lymphocyte gate showed high CD37 expression; CD37 expression was comparatively limited in other cells. The expression level of CD37 on the surface of single cells was evaluated quantitatively (Fig. 1B). High levels of CD37-sABC were detected in a subset of lymphocytes; comparatively low CD37-sABC was detected among the remaining lymphocytes, as well as neutrophils and monocytes (sABCs per cell for CD37: (high) lymphocytes, 91,600.0 ± 4,089.6; (low) other lymphocytes 2,917.7 ± 184.2; neutrophils, 3,612.4 ± 122.4; monocytes, 3,484.1 ± 166.1). CD37-high cells were confirmed as $CD19^+$ B lymphocytes (99.5–100.0%, $n = 5$; Supplemental Fig. 1A, 1B). We confirmed that only a part of $CD19^+$ cells were $CD37^+$ in PB leukocytes, whereas neutrophil, monocytes, and CD19-negative cells were weakly CD37 positive.

Although the CD37 expression in T cells under steady-state conditions has been examined, there are few data on changes in the CD37 expression under inflammatory conditions. Therefore, the transition of CD37 expression on $CD3^+$ T cells after CD3/CD28 stimulation was evaluated (Fig. 1C). The mean fluorescence intensity (MFI) ratio showed a slight, transient increase on the day after activation with CD3/CD28 beads; expression of CD37 returned to baseline within 24 h and remained constant thereafter.

CD37 expression during B cell differentiation was evaluated using BM samples from healthy donors (Fig. 1D). Differentiation into $CD19^+$ B cells was evaluated at four differentiation stages demarcated by expression of CD10 and CD45 Ags (43). In the fraction identified as early precursors (fraction A) through early intermediates (fraction B), CD37 expression was as low and could not be differentiated from those of other leukocyte lineage precursors; by contrast, we detected a significant increase in CD37 expression among late intermediate precursors (fraction C). Mature B cells in the BM (fraction D) expressed CD37 to the same extent as B cells in PB.

### *Generation of the CD37CAR construct and the impact of spacer length on the proliferation and viability of CAR-T cells*

To generate an effective CD37CAR construct, we created an scFv that included an L chain and an H chain based on the DNA sequence of the humanized anti-CD37 Ab (Supplemental Table I). The CD37CAR molecule was constructed by linking the spacer domain (the hinge and H chain C region), the CD28 TM domain, the CD28 intracellular domain, and CD3ζ signaling components to the scFv (Fig. 2A). Because there was a concern that the CAR-T cells might attack each other, as they themselves express CD37 weakly, we attempted to adjust the sensitivity of the CD37CAR by optimizing the length of the spacer domain (hinge and C region) that follows the anti-CD37 scFv. We created a series of CD37CAR molecules including one with no spacer (spacer length, 0 aa), in which scFv and CD28 TM domain are directly linked to one another without a spacer domain, to one with a 232-aa spacer that included the entire IgG4-derived hinge and C region; others including those with 15, 30, 60, and 125 aa were prepared. Because the size of IgG-Fc hinge is 15 aa and the length of CH2 domain and CH3 domain are 110 and 107 aa, we chose the size of twice the length of Fc hinge (30 aa) and further longer version to test the entire length of Fc-CH2-CH3 (232 aa). We found that the frequency of $tEGFR^+$ cells after gene transfer increased with increased spacer length (Fig. 2B). The number of CD37CAR-T cells decreased as the spacer length increased, although the differences observed did not reach statistical significance (Fig. 2C). Each of the six different lines of CD37CAR-T cells were purified, and proliferation was evaluated in response to activation with irradiated cells from the $CD37^+$ Ramos cell line. Low levels of proliferation were observed for the CD37CAR-T cells with the shortest and the longest spacers. The

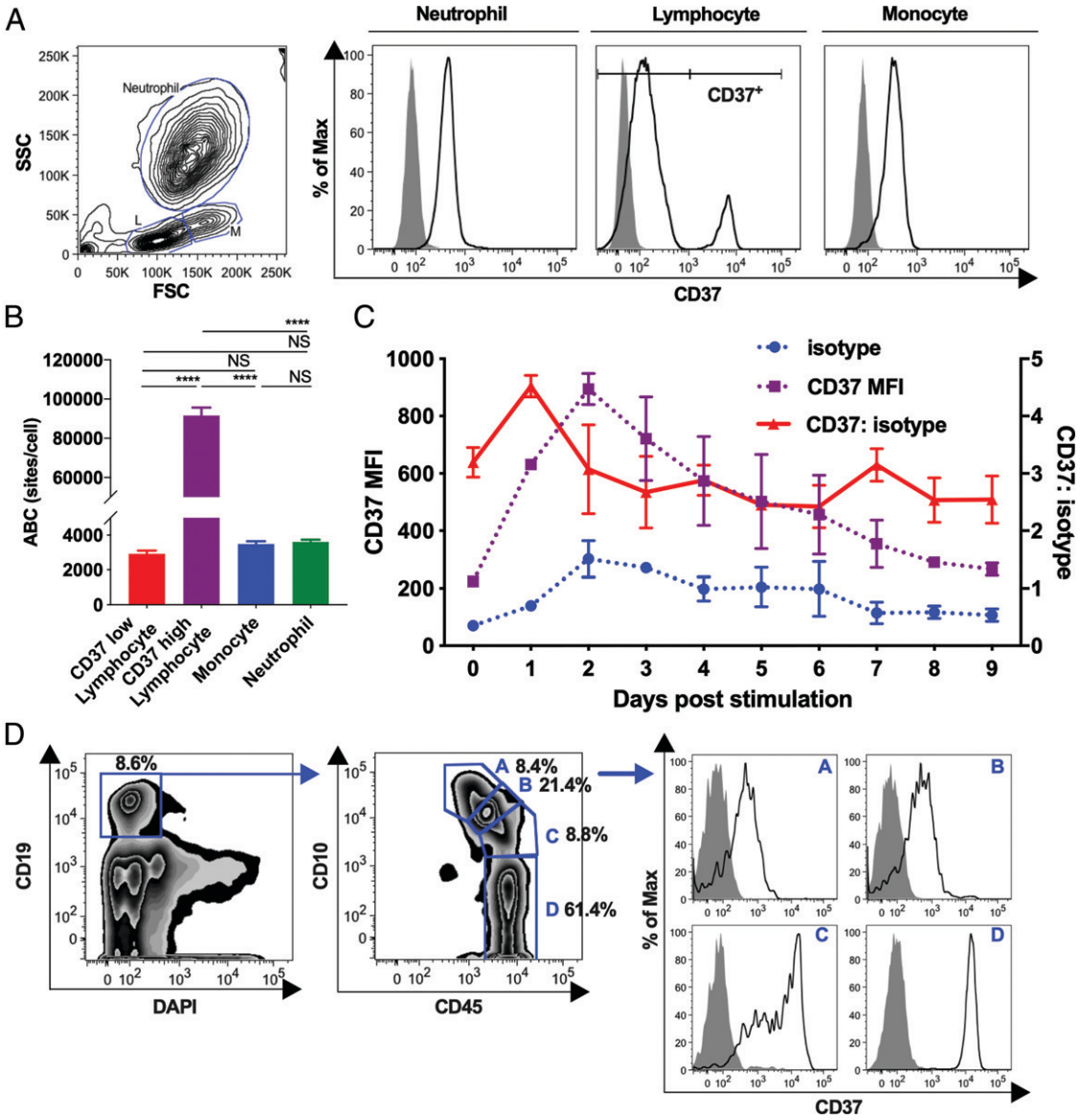


**FIGURE 1.** CD37 expression in normal leukocytes and activated T cells. (**A**) CD37 expression in leukocytes isolated from normal donor PB. Neutrophils, lymphocytes (L), and monocytes (M) were gated and analyzed for CD37 expression by flow cytometry. Gray histograms represent isotype control staining for each cell lineage. (**B**) CD37 expression was quantified as ABC by using a QIFIKIT. (**C**) CD37 expression in activated T cells. T cells were stimulated with CD3/CD28 beads on day 0, and surface expression of CD37 was determined. MFI of anti-CD37 and isotype staining were determined, and the ratio between the two (CD37/isotype) was calculated. (**D**) CD37 expression on B cell precursors in healthy donor BM. Normal donor BM was gated as DAPI-negative/CD19$^+$ fraction and further analyzed on the basis of differential expression of CD10 and CD45. Fraction A, early B cell precursor; fraction B, early intermediate B cell; fraction C, late intermediate B cell; fraction D, mature B cell. Gray histograms represent isotype control staining. Data are representative of three independent donor BM samples. Assays were performed on three biologically independent samples ($n = 3$) with data presented as mean ± SEM in (B) and (C). ****$p < 0.0001$, one-way ANOVA. NS, not significant.

CD37CAR-T lines with relatively short spacers (15 or 30 aa) proliferated most effectively (Fig. 2D). To investigate the association between spacer length and degree of T cell apoptosis/cytotoxicity, we performed annexin V/PI assay after coculture of CD37CAR-T with 0-, 15-, 125-, and 232-aa spacers and CD37 differentially expressed NALM6 (Supplemental Fig. 2A). We observed significant difference in apoptosis of CAR-T cells between CAR-T with shorter spacer (0 or 15 aa) and that with 232-aa spacer at 4 h poststimulation. At 8 h poststimulation, we observed significant difference in apoptotic cells between CAR-T with 15 aa and that with 232 aa except against CD37-high target. There was a clear tendency of higher apoptotic cell frequencies in CAR-T cells with longer spacer (Fig. 2E). In terms of target cell apoptosis, there were significant differences among CAR-T with different spacer length. In the earlier time point (4 and 8 h), the lower proportions of target cells were apoptotic with the shorter spacer CAR-T; however, the difference became smaller after 24 h of culture (Fig. 2F, Supplemental Fig. 2B).

To clarify whether the CAR-T cell enrichment during initiation culture was caused by fratricide, autologous T cells were cultured separately from CAR-T, which were then labeled with CTV and cocultured at a 1:1 ratio with CAR-T cells with different spacer lengths. Within 7AAD-negative live cell gate, we could clearly segregate target autologous T cells (CTV$^+$) and CAR-T/tEGFR-T cells (CTV$^-$) (Supplemental Fig. 2C). In the cultures with CD37CAR-T cells with longer spacer, we observed the lower frequencies of target cells within live cell

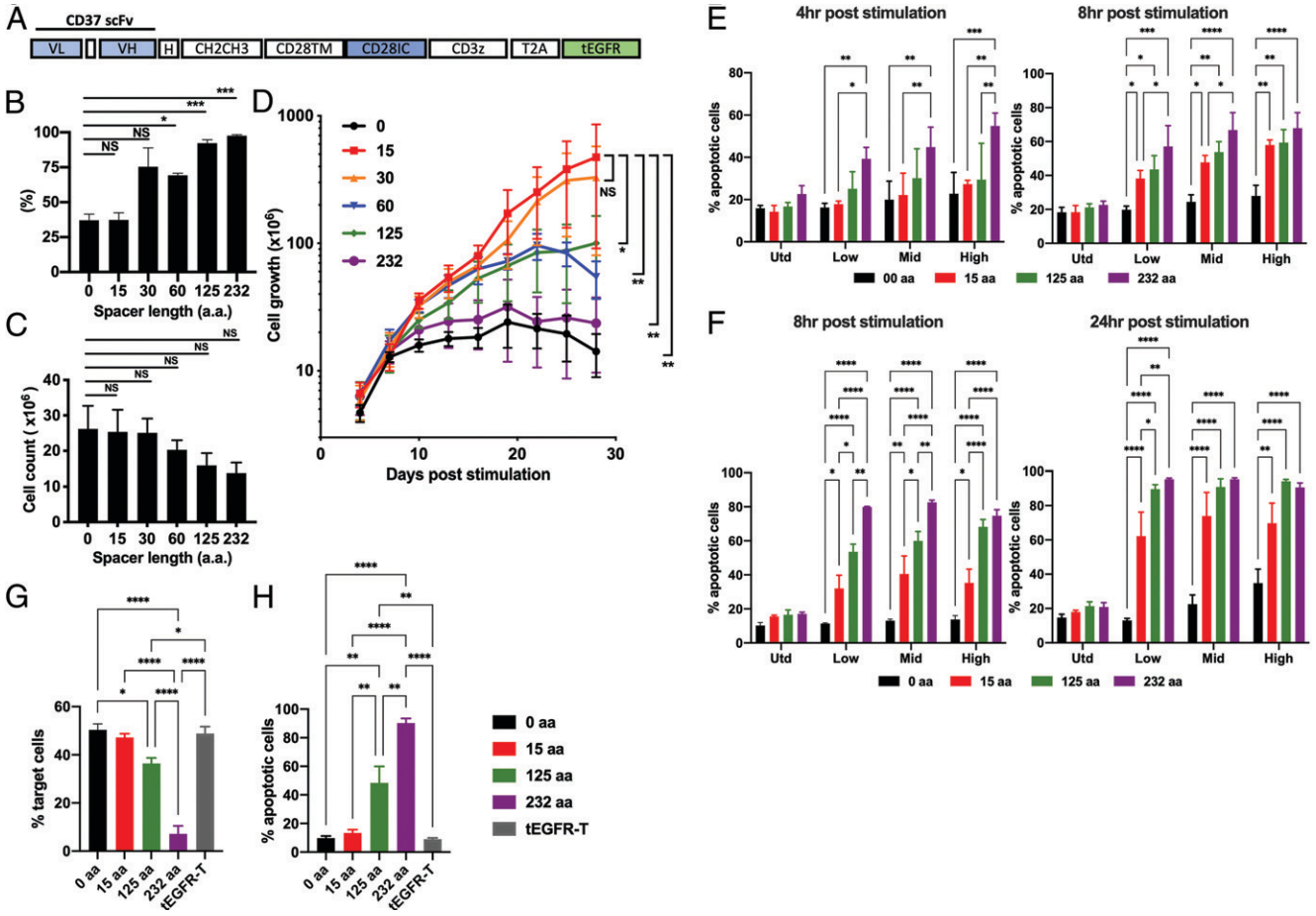


**FIGURE 2.** Construction of CD37CAR and effect of spacer length on CAR-T generation and proliferation. (**A**) Schematic representation of CD37CAR. A CD28 costimulatory domain was linked to anti-CD37 scFv-H/$CH_2CH_3$-CD28 TM domain, followed by CD3ζ and tEGFR. CH, H chain C region; H, IgG4-derived hinge; VH, H chain variable fragment; VL, L chain variable fragment. (**B**) Transduction efficiency of CD37CAR after a single course of transduction culture with cells from five different donors. $CD3^+$ lymphocytes were purified by immunomagnetic beads; these cells were transduced with CD37CAR, and the frequencies of $CAR^+$ cells were assessed. Percentages of $CAR^+$ cells were determined from $tEGFR^+$ cells from within the lymphocyte gate. All findings represent mean ± SEM. $*p < 0.05$, $***p < 0.001$, one-way ANOVA. (**C**) CD37CAR-transduced cell count after one course of transduction. Cell numbers were determined by multiplying live cell count by the percentage of $tEGFR^+$ cells. Data represent means ± SEM from five different donors. No significant differences were observed (one-way ANOVA). (**D**) CD37CAR-T cell proliferation after stimulation. CD37CAR-T cells were purified and stimulated once with γ-irradiated Ramos cells at a 1:5 ratio and cultured with IL-2 supplementation (50 IU/ml). T cell expansion was measured by counting viable cells. Results at day 28 from five different donors were shown. $*p < 0.05$, $**p < 0.01$, two-way ANOVA. (**E**) CAR-T apoptosis after 4 and 8 h coculture with CD37 differentially expressed NALM6 cell lines. (**F**) NALM6 apoptosis after 8 and 24 h coculture. Percentages of apoptotic CAR-T cells and NALM6 (annexin $V^+/PI^-$ and annexin $V^+/PI^+$) are shown from three different donors (one-way ANOVA). (**G** and **H**) Autologous T cells were cultured separately from CAR-T, which were then labeled with CTV and cocultured for 24 h at a 1:1 ratio with CAR-T cells with different spacer lengths. (G) $CTV^+$ target cells within 7AAD-negative live cell gate and (H) apoptotic cells within all $CTV^+$ cells (one-way ANOVA). Significance levels were shown only for the comparisons with significance. (E–H) $*p < 0.05$, $**p < 0.01$, $***p < 0.001$, $****p < 0.0001$.

gate (Fig. 2G) and the higher frequencies of apoptotic cells within $CTV^+$ target cells (Fig. 2H).

### *Signaling after CD37 stimulation among CD37CAR-T cells with different spacer length*

To investigate the proximal and distal signaling after target Ag binding, we performed intracellular phospho-flow analysis. A short 5-min stimulation induced only small phosphorylation of CD3ζ in the CD37CAR-T cells, whereas both the proportion of T cells with phosphorylation of p38 and ERK and the MFI of staining were the highest in the CD19CAR-T cells and the lowest in the CD37CAR-T with 15-aa spacer (Fig. 3A–D). The background phosphorylation level was lower in the CD37CAR-T cells compared with CD19CAR-T cells (Fig. 3B). Taken together, by varying the spacer length of CD37CAR-T, we could suppress fratricide in the early culture and activation induced cell death and maintain cell proliferation after CD37 stimulation. The phosphorylation signal was attenuated by shortening the length of the spacer. Accordingly, we used the CD37CAR line with the 15-aa spacer for all further experiments performed in vitro and in vivo.

### *Cytokine secretion, cytotoxic function, and T cell proliferation upon activation of $CD37^+$ cells*

To explore the basic functions of CD37CAR-T cells in vitro, $CD8^+$ T cells of healthy donors were retrovirally transduced and evaluated. The gene transduction efficiency was ∼60 and 80% for control tEGFR-transduced and CD37CAR-transduced T cells, respectively (Fig. 4A). After cell purification using tEGFR, the percentage of isolated T cells that expressed CD37CAR achieved 95–100% (Fig. 4A).

CD37CAR-T cells produced IFN-γ only after stimulation with $CD37^+$ cells (Fig. 3B). CD37CAR-T cells responded with robust production of IFN-γ and IL-2 upon CD37-mediated stimulation (Fig. 4C, 4D). A coculture assay was conducted to evaluate the cytotoxic activity and cell proliferation of CD37CAR-T cells. CD37CAR-T cells suppressed the proliferation of Raji-ffluc cells

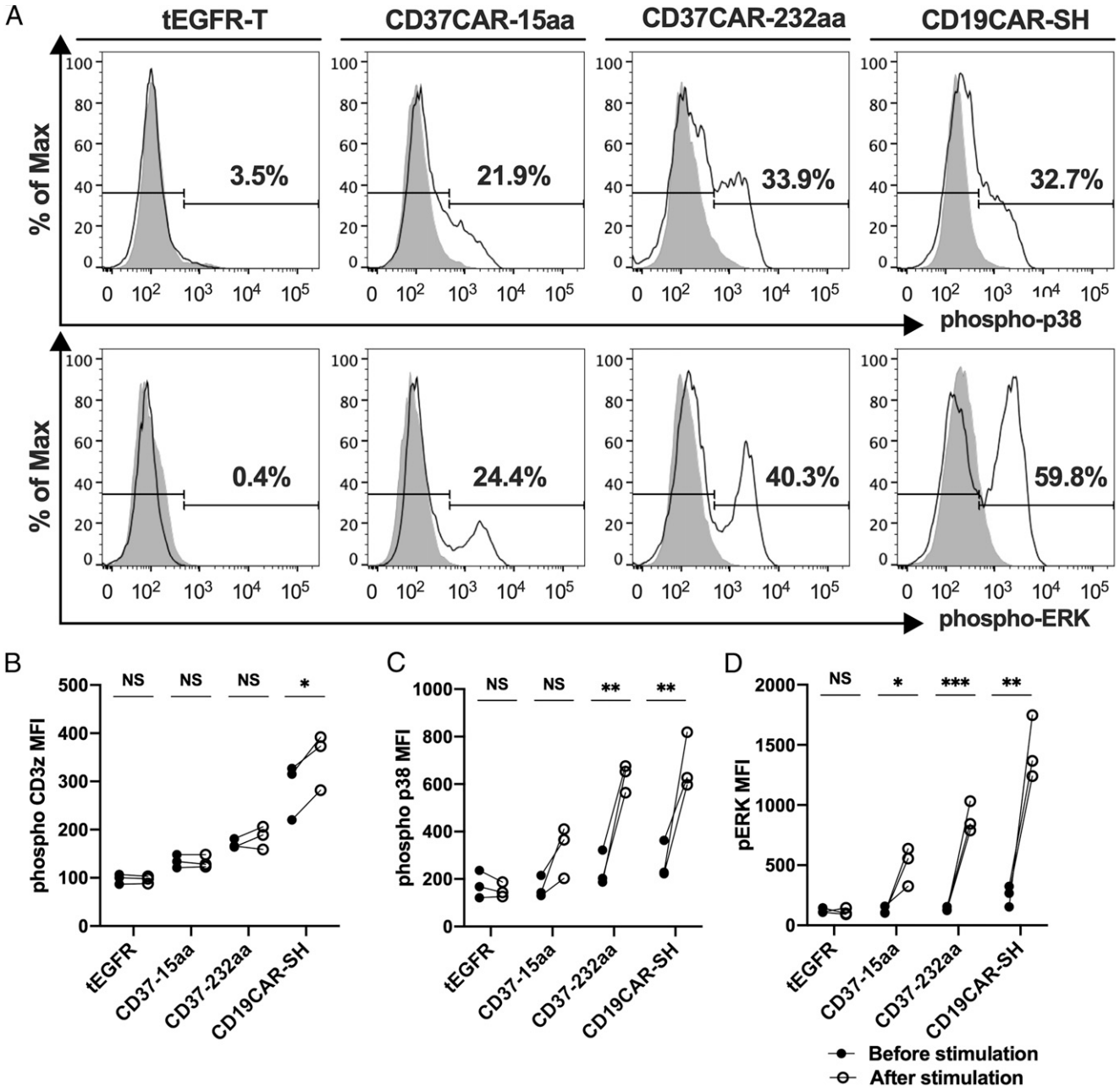


**FIGURE 3.** Analysis of intracellular signaling after stimulation through the CAR. (**A**) Intracellular phospho-specific staining of p38 and ERK. CAR-T cells and tEGFR-T cells were stimulated with Raji tumor cells at a 1:5 ratio for 30 min. Data are representative of three independent experiments with three donors. (**B**–**D**) MFI data before and after stimulation of phospho-CD3ζ (B), phospho-p38 (C), and phospho-ERK (D). $*p < 0.05$, $**p < 0.01$, $***p < 0.001$, paired *t* test.

during the observation period (Fig. 4E, 4F). CD37CAR-T cell proliferation after stimulation was evaluated both with and without IL-2. We found that CD37CAR-T cells were activated by irradiated Raji cells and grew to 15–20 times without IL-2 and to 60–80 times in the presence of IL-2 (Fig. 4G, 4H).

*Association between CD37 expression and cytotoxicity by CD37CAR-T cells*

CD37 expression in tumor cell lines derived from various leukocyte lineages, including B cell lymphomas, was assessed (Fig. 5A). Tumor cell lines derived from B cell lymphomas, including Burkitt lymphoma, were characterized by relatively high CD37 expression. Cell lines derived from multiple myeloma and B-ALL came from tumors that originally expressed minimal or no CD37 expression but currently demonstrate moderate CD37 expression. Tumor cell lines derived from acute myeloid leukemia were weak $CD37^{+}$.

Cells from the various tumor cell lines were labeled with CFSE, mixed 1:1 with CD37CAR-T cells, and cocultured for 72 h. Coculture with control $tEGFR^{+}$ T cells resulted in survival and ongoing increase in the number of tumor cells, whereas coculture with CD37CAR-T cells suppressed the growth of tumor cell lines that expressed even minimal quantities of CD37 (Fig. 5B). Tumor cell lines that were clearly CD37 negative were not inhibited in response to coculture with CD37CAR-T cells. Of note, we observed growth suppression of tumor cells that expressed CD37 at lower levels than PB T cells, neutrophils, and monocytes. Tumor cell lines with lower

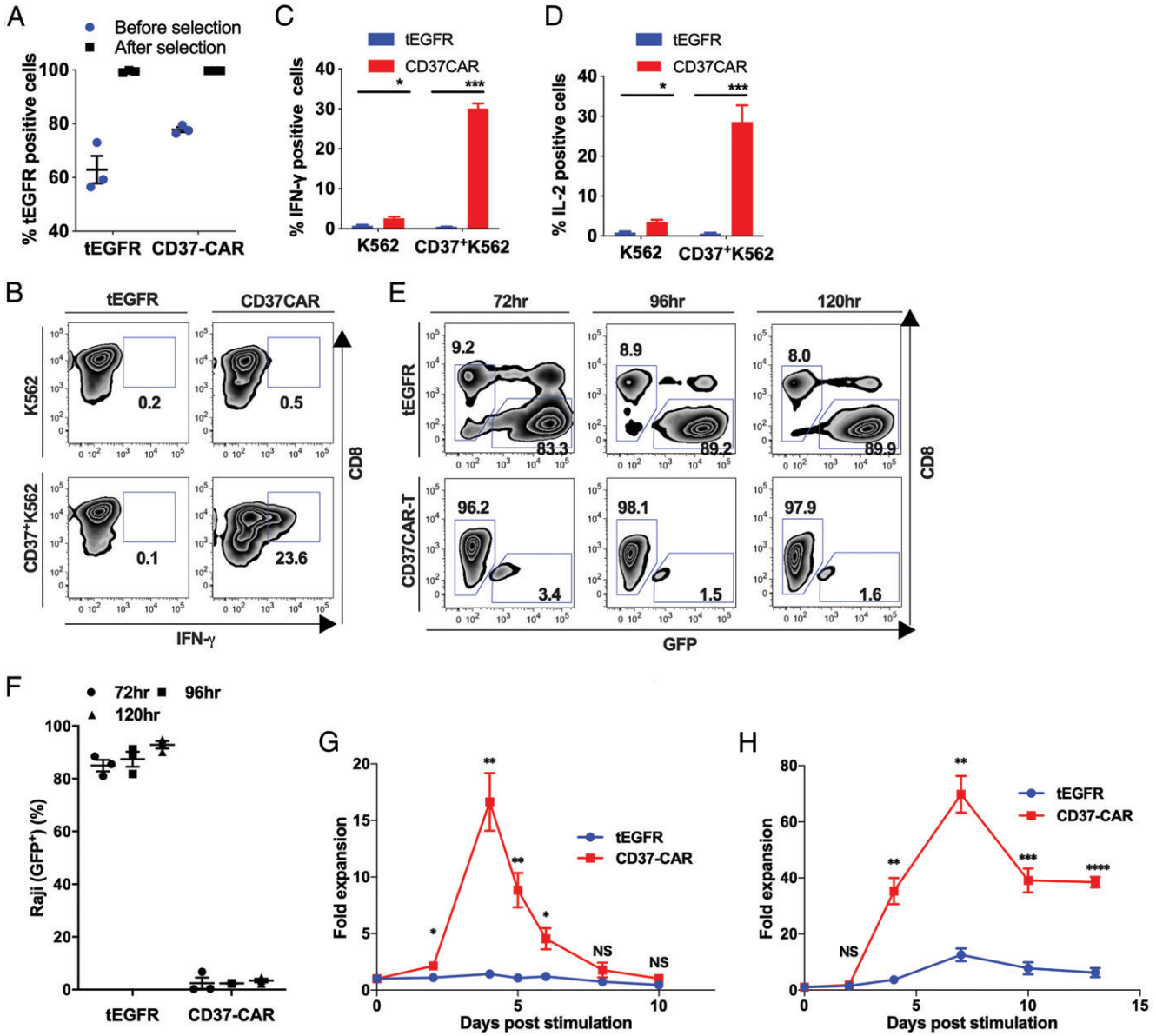


**FIGURE 4.** Cytokine secretion, cytotoxic function, and T cell proliferation upon $CD37^+$ target cell stimulation. (**A**) Transduction and purification efficiency of CD37CAR-T cells. After transduction, CD37CAR-T cells were purified with biotinylated anti-EGFR mAb and anti-biotin microbeads. Percentages before and after tEGFR purification were determined by staining with anti-EGFR. (**B–D**) Intracellular IFN-γ– or IL-2–positive cells after stimulation with $CD37^+$K562 cells. Purified CD37CAR-T cells or $tEGFR^+$ cells were stimulated with $CD37^+$K562 cells at an E:T ratio of 1:1 for 4 h; cells were then permeabilized and stained for intracellular IFN-γ or IL-2. Representative flow plots are shown in (B), and summarized data from three different donors are shown in (C) and (D). (**E**) CD37CAR-T cells were cocultured with live Raji-ffluc cells to assess their impact on both cytotoxicity and proliferation at an E:T ratio of 1:1 for a total of 120 h; the percentage of remaining Raji cells was assessed every 24 h by flow cytometry. Representative flow plots are shown. (**F**) Coculture findings from three unrelated donors. The frequencies of target tumor cells fraction were obtained by flow cytometry as shown in (E). (**G** and **H**) Proliferation in response to single Ag stimulation was assessed using standard trypan blue dye exclusion (G) without or (H) with IL-2 supplementation (50 IU/ml) every 3 d. In 12-well tissue culture plates, $5 \times 10^5$ CD37CAR-T cells or control $tEGFR^+$ T cells were stimulated with $5 \times 10^5$ γ-irradiated Raji cells ($CD37^+$). The number of live T cells was assessed using standard trypan blue dye exclusion. Findings are from three independent donors and presented as mean ± SEM. *$p < 0.05$, **$p < 0.01$, ***$p < 0.001$, ****$p < 0.0001$, Student $t$ test was performed to evaluate each time point.

levels of CD37 expression than those detected on OCI–Ly-10 cells did not show complete CD37CAR-T–mediated tumor cell growth inhibition. Of these, U266H, NALM6, and SUP-T1 demonstrated no CD37CAR-T–mediated growth suppression, whereas other $CD37^{low}$ cell lines showed detectable suppression (Fig. 5B).

### *Recognition of CD37 on normal leukocyte lineages in vitro and in vivo*

Given the aforementioned findings, there is significant concern that CD37CAR-T cells may exhibit cytotoxic activity against healthy leukocytes and thereby promote adverse events in CD37CAR-T cell therapy. To investigate CD37CAR-T cell function with respect to healthy PB leukocytes, $CD37^{high}$ lymphocytes, and $CD37^{low}$ lymphocytes, monocytes, and neutrophils were obtained from PBMCs of healthy donors, and cytotoxic activity was investigated with 4-h standard chromium release assay (Fig. 6A), and cytokine production was evaluated (Fig. 6B, 6C). Whereas we observed significantly higher cytotoxic activity against $CD37^+$K562 and $CD19^+$ B cells, we further observed weaker but significant cytotoxicity against K562, $CD3^+$ T cells, and monocyte (Fig. 6A). Compared with T cells

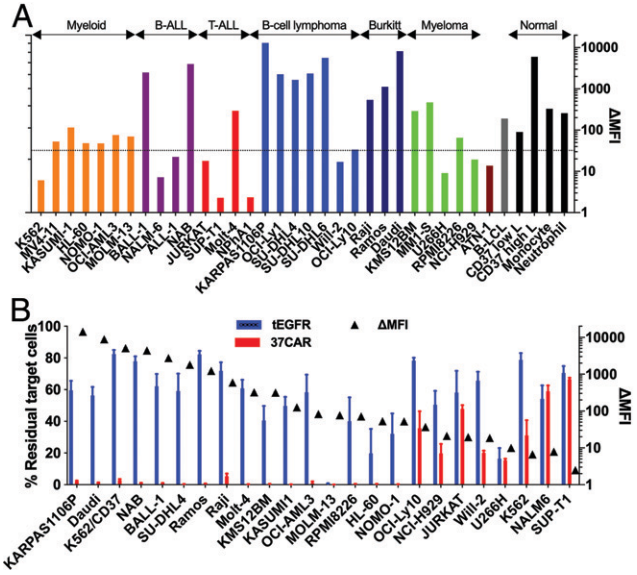


**FIGURE 5.** Association between CD37 expression and CD37CAR-T cell–mediated cytotoxicity. (**A**) CD37 expression of various tumor cell lines and normal leukocyte lineages in PB. CD37 expression was analyzed with flow cytometry. Burkitt, Burkitt lymphoma; T-ALL, T cell acute lymphoblastic leukemia. CD37 ΔMFI was calculated as CD37 MFI minus the MFI determined for the matched isotype. Dashed line was drawn at MFI determined for OCI–Ly-10. Data are representative of three repeated experiments including normal PB cells from three independent donors. (**B**) Coculture assays with various tumor cell lines targeted by tEGFR$^+$ T cells or CD37CAR-T cells. Various tumor cell lines as described in (A) were labeled with CFSE and mixed with purified tEGFR$^+$ or CD37CAR-T cells at a 1:1 ratio. After 72-h incubation and T cell staining, percentages of residual tumor cells were determined within the live cell gate and listed in order of CD37 ΔMFI (triangles). Data presented are from the analysis of three independent donors and presented as mean ± SEM.

expressing tEGFR only, CD37CAR-T cells resulted in significantly higher cytokine production against the CD37$^{high}$ lymphocytes; this was not observed after the stimulation with CD37$^{low}$ lymphocytes, monocytes, or neutrophils. However, the extent of cytokine production that resulted from CD37CAR-T activation by CD37$^{high}$ lymphocytes was lower than that detected after the stimulation with the CD37$^+$K562 (Fig. 6B, 6C).

To explore the potential influence of CD37CAR-T cells on human BM cells, we created humanized mice that can be used to test in vivo impact against human BM cells. After 12 wk of cord blood–derived CD34$^+$ cells injection, tEGFR$^+$ T cells or CD37CAR-T cells were injected i.v.; mouse BM cells were collected and evaluated both before and after this event (Fig. 6D). The percentage of hCD45$^+$ cells remained unchanged in response to injection (Fig. 6E). CD37 expression on hCD3$^+$, hCD19$^+$, hCD33$^+$, and hCD34$^+$ cell fractions before and after injection of CD37CAR-T cells was evaluated in the BM of humanized mice (Fig. 6F). We observed no apparent changes in CD37 expression among the hCD3$^+$, hCD33$^+$, and hCD34$^+$ cells. Furthermore, among the hCD19$^+$ cells, the CD37$^{hi}$ fraction detected in BM prior to the CD37CAR-T cell injection disappeared in response to this treatment; the responses of this fraction corresponded with those of mature B cells in PB of healthy donors. From these results, we conclude that only normal leukocytes targeted by CD37CAR-T cells were CD37$^{hi}$ cells among CD19$^+$ fraction. When CD19CAR-T cells were i.v. injected into the humanized mice, hCD19$^+$ cells completely disappeared from the BM. By contrast, when the CD37CAR-T cells were injected i.v., we could still detect the hCD19$^+$ cell population, and expression of CD37 in these hCD19$^+$ cells also remained unchanged (Fig. 6G).

*Antitumor activity of CD37CAR-T cells*

Because CD37CAR-T cells did not target human PB cells with weak CD37 expression, we evaluated CD37CAR-T cell responses to patient-derived tumor cells. Two patient-derived samples from patients diagnosed with DLBCL were confirmed as CD19$^+$, CD20$^+$, and CD37$^+$ (Fig. 7A). CD37CAR-T cells produced both IFN-γ and IL-2 after tumor cell stimulation; the production observed was robust even when compared with that resulting from stimulation with CD19CAR-T cells (Fig. 7B, 7C, Supplemental Fig. 3).

To explore the antitumor effect of CD37CAR-T cells in vivo, we performed xenograft experiments with NOG mice inoculated with Raji-ffluc cells (Fig. 8A, 8B). Injection of CD19CAR-T or CD37CAR-T cells resulted in significant suppression of Raji growth in NOG mice (Fig. 8C); introduction of CD37CAR-T cells resulted in prolonged survival of NOG mice with Raji-ffluc tumors compared with results from controls (Fig. 8D).

## Discussion

To improve treatment efficacy for hematological malignancies, we developed CD37CAR-T cells. CD37 is a membrane protein belonging to the tetraspanin superfamily and is exclusively expressed in immune cells (14, 16, 18, 19). CD37 is highly expressed in mature B cell and in B cell malignancies; CD37 expression has also been detected in some T cell malignancies. Because the Ag affinity of the CAR molecule is generally quite high, there has been concern that CD37CAR-T cells might be cytotoxic for endogenous T cells that express low levels of CD37. To achieve both antitumor efficacy and safety, we first evaluated CD37 expression in normal leukocyte lineages.

There are various factors that influence the function of the CAR molecule; the affinity of the Ag recognition region of scFv is of course of major concern (44–46); however, it is also critical to explore the impact of the location of the scFv epitope within the target Ag (47) and the type and number of costimulatory domains (48–50). Proven strategies for avoiding fratricide include methods that can knock down the target Ag on T cells and/or use of epitopes that target a conformation identified only in tumor cells (47, 51, 52). In this study, we focused on the length of the spacer domain. We found that the length of the spacer has a clear impact on the capacity of the CD37CAR molecule to recognize CD37 and to proliferate in response to CD37-mediated activation (31–33). Specifically, we found that a very small spacer reduced gene transfer efficiency and limited the proliferation of transduced CAR-T cells. By contrast, a very long spacer also resulted in poor proliferation of the CAR-T–transduced cells. The differences in the rates of proliferation may be because CAR-T cells with a longer spacer are more capable of associating with a larger number CD37 Ags on target cells and, thus, are more efficient at fratricide. We observed the higher rate of apoptotic CAR-T cells in longer spacer CD37CAR-T, which was further higher against CD37-mid or -high NALM6 cells; the mechanism for the difference was mainly due to the attenuated signaling mediated by the shorter spacer CAR-T. We consider that the long spacer CAR could ligate with a wider range of target Ag within immunological synapse and mediate stronger signals, resulting in the apoptosis in the longer spacer CAR-T cells. Thus, we hypothesized that the CD37CAR-T with longer spacer may exhibit more robust immunological synapse (53); we have attempted to capture a sense of this synapse by immunofluorescence staining, but thus far, our results have been inconclusive. Because CD37 is known to be extensively glycosylated glycoprotein, differential glycosylation of

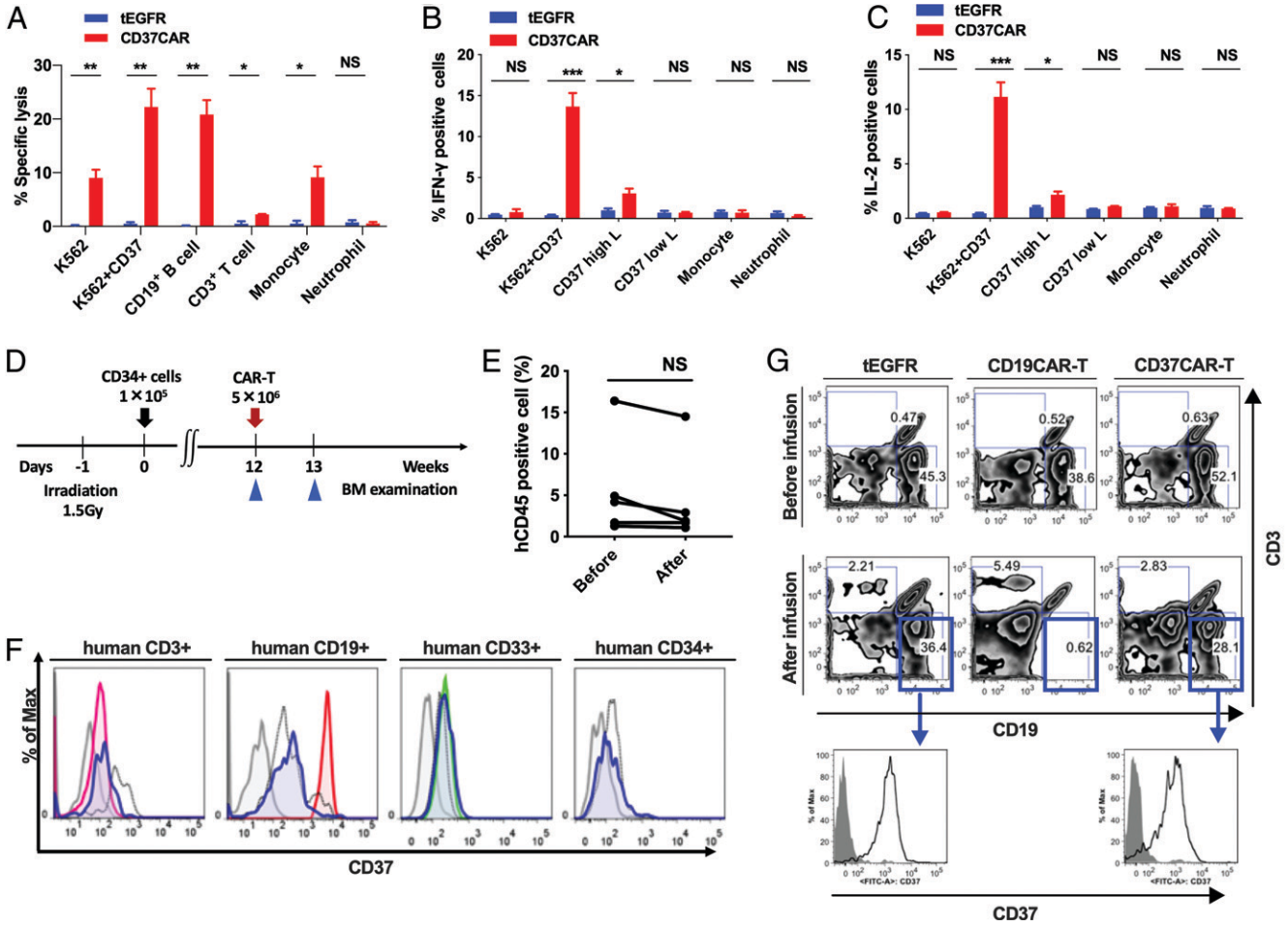


**FIGURE 6.** Recognition of CD37 on normal leukocytes in vitro and in vivo. (**A**) tEGFR$^+$ and CD37CAR-T cell cytotoxicity against K562, CD37$^+$K562, and normal leukocyte fractions. (Standard chromium release assay at E:T ratio of 1:1.) Data are summarized from three independent donor CD37CAR-T cells. (**B** and **C**) tEGFR$^+$ and CD37CAR-T cells positive for intracellular IFN-γ and IL-2 after stimulation with K562, CD37$^+$K562 cells, or normal leukocytes. Purified CD37CAR-T cells or tEGFR$^+$ cells were stimulated with flow-sorted or bead-purified normal PB-derived cells at an E:T ratio of 1:1 for 4 h then permeabilized and stained for intracellular IFN-γ (B) and IL-2 (C). Data are summarized from three independent donors. $*p < 0.05$, $**p < 0.01$, $***p < 0.001$, Student $t$ test. (**D**) Schematic representation of the in vivo experimental design. After irradiation with 1.5 Gy on day −1, NOG mice were inoculated with $1 \times 10^5$ cord blood CD34$^+$ cells via tail vein injection on day 0. Twelve weeks later, after human-derived hematopoiesis was confirmed, mice received either $5 \times 10^6$ tEGFR-transduced or CD19CAR-T or CD37CAR-T cells. BM samples were analyzed before and after T cell infusion for frequencies of hCD45$^+$ as well as CD3$^+$, CD19$^+$, CD33$^+$, and CD34$^+$ cell fractions. (**E**) Percentages of hCD45$^+$ cell in BM of the humanized mice. Shown are frequencies within live cell gate (paired $t$ test). (**F**) Representative flow plots of CD37 expression before and after CD37CAR-T cell infusion. Gray histograms represent isotype staining; dotted lines represent expression prior to infusion, and blue lines are after infusion. Pink, red, and green lines represent normal levels of CD3$^+$, CD19$^+$, and CD33$^+$ cells from donor PB, respectively. Shown are representative results from two different cord blood sources, and each condition contained two to three mice (total of five mice for CD37CAR-T infusion). (**G**) Representative flow plots of CD3$^-$CD19$^+$ fraction and CD37 expression. Frequencies of hCD45$^+$ cells and CD3$^-$CD19$^+$ cell fraction were determined as described in (E). CD37 expression on cells in the CD3$^-$CD19$^+$ fraction after CD19CAR-T infusion cannot be included, as only a limited number of cells were available. Gray histograms represent isotype staining; black lines are CD37 expression after infusion.

CD37 on normal and malignant hematopoietic cells may be another possible mechanism (54). Two previous papers reported that they did not observe any significant fratricide during the development of CD37CAR-T cells (35, 36). We would be very interested to explore the differences between the two preparations of CD37CAR-T cells. For the remaining experiments, we used CD37CAR-T cells with a moderate-sized spacer.

CD37 was weakly expressed in T cells isolated from PB of healthy donors, as described previously (20). Because CAR-T cells are activated by stimulation with the target Ag, we evaluated the CD37 expression in the activated T cells. We observed a transient increase in CD37 expression on activated T cells shortly after stimulation; CD37 levels then returned to baseline levels that were comparable with those of unstimulated T cells. It is important to recognize increased levels of CD37 expression were still much lower than those detected on B cells; as such, we anticipated that the transient CD37 upregulation would not result in self-destruction of the larger CD37CAR-T cell population. However, to the best of our knowledge, no data have examined CD37 expression in strong inflammatory conditions such as graft-versus-host disease, and it remains possible that CD37CAR-T may recognize upregulated CD37 in the strong inflammatory conditions. We also examined CD37 expression during B cell maturation in the BM. CD19 is also strongly expressed in immature B cells. CD37 expression increases gradually with B cell maturation; CD37$^+$ cells can be detected in the CD19$^+$ cell fraction. We anticipate that the effect of CD37CAR-T cells on normal B cells would be somewhat less than that of CD19CAR-T cells.

From the viewpoint of the safety, it will be important to make CAR-T cells not to recognize normal cells (30). To

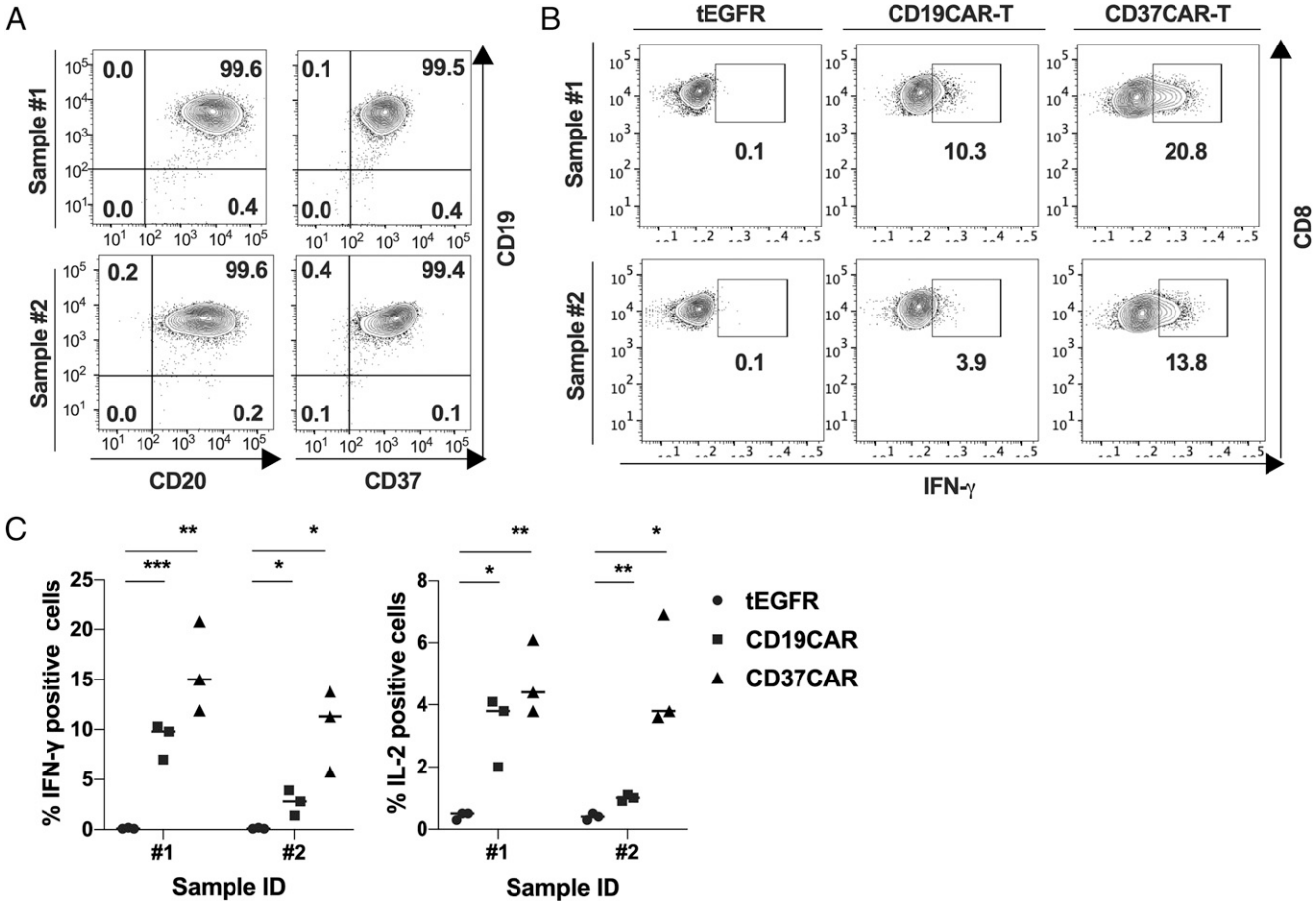


**FIGURE 7.** CD37CAR-T cells recognize patient-derived tumor cells. (**A**) Expression of CD19, CD20, and CD37 on patient-derived tumor cells. Dead cells were removed after thawing. Sample 1 was derived from a patient diagnosed with DLBCL, and sample 2 was from a patient with double-hit lymphoma. (**B** and **C**) Intracellular IFN-γ–positive cells after stimulation with patient-derived tumor cells. Purified tEGFR$^+$ cells, CD19CAR-T cells, or CD37CAR-T cells were stimulated with tumor cells at an E:T ratio of 1:1 for 6 h and then permeabilized and stained for intracellular IFN-γ in (B) and for intracellular IL-2 as shown in Supplemental Fig. 2. Representative flow plots are shown in (B) and in Supplemental Fig. 2. Representative flow plots are shown in (B) and in Supplemental Fig. 2. The data are summarized from three independent donors as shown in (C). Each dot represents the result from a single donor. $*p < 0.05$, $**p < 0.01$, $***p < 0.001$, paired $t$ test.

evaluate the potential effect on the normal leukocytes, PB cells isolated from healthy donors were cocultured with CD37CAR-T cells, and cytotoxic activity and cytokine production were analyzed. CD37CAR-T–mediated cytotoxic activity was demonstrated against CD37-high cells such as CD37$^+$K562 and CD19$^+$ B cells and other CD37-low cells (K562, CD3$^+$ T cell, and monocyte). In terms of cytokine production, we observed significant cytokine production for B cells that expresses high levels of CD37, whereas we observed no significant response to other leukocyte lineages. Although cytotoxic activity as an immediate response was seen against some normal cells, this response was not reflected in cytokine production. The responses to normal B cells were not strong compared with those observed to tumor cell lines that express CD37 at high levels. Although there remain concerns regarding the potential for CD37CAR-T cell fratricide and, likewise, cytotoxic activity on normal PB leukocytes, we observed no evidence suggesting that our cell preparations targeted anything other than B cells. In addition, mice that were reconstituted with hCD34$^+$ progenitor cells so as to mimic human hematopoiesis were created to evaluate the effect of CD37CAR-T cells on human BM function (41). Although CD19CAR-T cells clearly targeted the CD19$^+$ cells in the BM of humanized mice, CD37CAR-T cells had no clear impact on this population, which maintained low levels of hCD37 expression throughout. As expected, when comparing BM before and after CD37CAR-T infusion, only the human B cells that expressed high levels of CD37 had disappeared. Taken together, our results suggest that the impact of CD37CAR-T cells on normal BM function might be smaller than that observed in response to CD19CAR-T cells. These results are consistent with previous reports that have also shown that CD37CAR-T cells have little effect on normal leukocytes (35).

By optimizing the spacer length, we have developed CD37CAR-T cells that maintain the antitumor effect while minimizing the impact on normal cells. In a study in immunodeficient mice, CD37CAR-T cells strongly suppressed the growth of transplanted Raji cells and prolonged the survival time of xenografted mice, although its capacity to inhibit tumor cell growth was slightly inferior to that of CD19CAR-T cells. This might be the result of very low levels of fratricide associated with self-ligation of CD37 by CD37CAR molecules on the surface of T cells. Because CD37CAR-T cells with shorter spacer exhibited attenuated signaling after CD37 Ag binding, insufficient signaling and activation would be possible explanation for the inferior in vivo function to the CD19CAR-T cells.

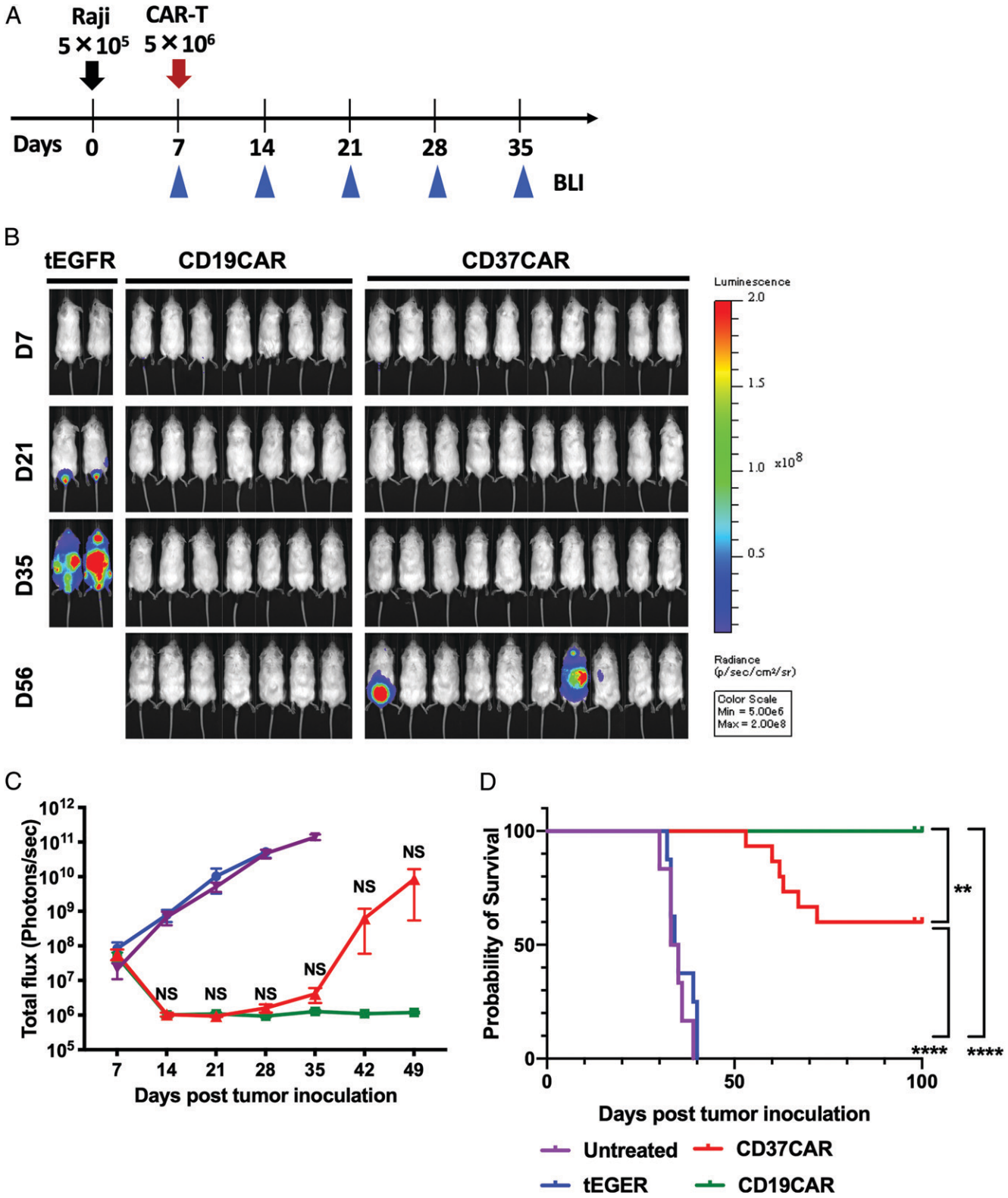


**FIGURE 8.** In vivo antitumor activity of CD37CAR-T cells. (**A**) Schematic of the in vivo experimental design. NOG mice were inoculated with $5 \times 10^5$ Raji-ffluc cells via tail vein injection on day 0. On day 7, mice received $5 \times 10^6$ nontransduced T cells, tEGFR-transduced T cells, CD19CAR-T cells, or CD37CAR-T cells. The tumor burden of each mouse was then evaluated via weekly bioluminescent imaging. (**B**) Bioluminescence of mice receiving different treatments. Shown are representative experiments of genetically modified T cells from two different donors ($n = 2$ for tEGFR-transduced T cell, $n = 7$ for CD19CAR-T cells, and $n = 10$ for CD37CAR-T cells). (**C**) Summary of tumor flux in each treatment group over time, following inoculation of Raji-ffluc cells. Data plotted as mean ± SEM. Statistics were performed among each treatment arm; the comparison between the CD19CAR-T and the CD37CAR-T cell groups are displayed (one-way ANOVA in each time point). (**D**) Kaplan–Meier plots of the survival of mice treated with genetically modified T cells. Mice treated with CD19CAR-T and CD37CAR-T cells showed significantly prolonged survival compared with mice treated with tEGFR-transduced T cells or untreated mice. Data were pooled from four independent experiments with gene-modified T cells from four donors, including 6–15 mice per group in (C) and (D). $^{**}p < 0.01$, $^{****}p < 0.0001$, log-rank test.

In summary, we have developed, to our knowledge, new CD37CAR-T cells for use in cancer immunotherapy. Because CD37 is expressed not only in mature B cell tumors but also in several T cell tumors, there is the possibility that this single agent may be useful for the treatment of several types of tumors. In addition, although CD37 is weakly expressed in normal leukocytes and on CAR-T cells themselves, optimizing the spacer length minimized fratricide while maintaining the antitumor effect. Modulation of spacer length may also be applied to other Ags identified for future applications of CAR-T cell therapy.

## Acknowledgments

The authors thank the Division of Experimental Animals and the Division of Medical Research Engineering, Nagoya University Graduate School of Medicine, for technical assistance.

## Disclosures

H.K. reports grants from Chugai Pharmaceutical, Kyowa Kirin, Zenyaku Kogyo, FUJIFILM, Otsuka Pharmaceutical, Takeda Pharmaceutical, Sumitomo Dainippon Pharma, Sanofi, Celgene, Nippon Shinyaku, Eisai, and Pfizer Japan; grants and personal fees from Daiichi Sankyo, Astellas, and Novartis Pharma; and personal fees from Bristol-Myers Squibb and Amgen Astellas BioPharma that are all unrelated to the submitted work. The other authors have no financial conflicts of interest.

## References

1. Ramchandren, R., E. Domingo-Domènech, A. Rueda, M. Trněný, T. A. Feldman, H. J. Lee, M. Provencio, C. Sillaber, J. B. Cohen, K. J. Savage, et al. 2019. Nivolumab for newly diagnosed advanced-stage classic Hodgkin lymphoma: safety and efficacy in the phase II CheckMate 205 study. *J. Clin. Oncol.* 37: 1997–2007.
2. Kochenderfer, J. N., M. E. Dudley, S. H. Kassim, R. P. Somerville, R. O. Carpenter, M. Stetler-Stevenson, J. C. Yang, G. Q. Phan, M. S. Hughes, R. M. Sherry, et al. 2015. Chemotherapy-refractory diffuse large B-cell lymphoma and indolent B-cell malignancies can be effectively treated with autologous T cells expressing an anti-CD19 chimeric antigen receptor. *J. Clin. Oncol.* 33: 540–549.
3. Maude, S. L., N. Frey, P. A. Shaw, R. Aplenc, D. M. Barrett, N. J. Bunin, A. Chew, V. E. Gonzalez, Z. Zheng, S. F. Lacey, et al. 2014. Chimeric antigen receptor T cells for sustained remissions in leukemia. *N. Engl. J. Med.* 371: 1507–1517.
4. Porter, D. L., B. L. Levine, M. Kalos, A. Bagg, and C. H. June. 2011. Chimeric antigen receptor-modified T cells in chronic lymphoid leukemia. *N. Engl. J. Med.* 365: 725–733.
5. Marcus, R., A. Davies, K. Ando, W. Klapper, S. Opat, C. Owen, E. Phillips, R. Sangha, R. Schlag, J. F. Seymour, et al. 2017. Obinutuzumab for the first-line treatment of follicular lymphoma. *N. Engl. J. Med.* 377: 1331–1344.
6. Mohty, M., J. Gautier, F. Malard, M. Aljurf, A. Bazarbachi, C. Chabannon, M. A. Kharfan-Dabaja, B. N. Savani, H. Huang, S. Kenderian, et al. 2019. CD19 chimeric antigen receptor-T cells in B-cell leukemia and lymphoma: current status and perspectives. *Leukemia* 33: 2767–2778.
7. Srivastava, S., and S. R. Riddell. 2018. Chimeric antigen receptor T cell therapy: challenges to bench-to-bedside efficacy. *J. Immunol.* 200: 459–468.
8. Maude, S. L., T. W. Laetsch, J. Buechner, S. Rives, M. Boyer, H. Bittencourt, P. Bader, M. R. Verneris, H. E. Stefanski, G. D. Myers, et al. 2018. Tisagenlecleucel in children and young adults with B-cell lymphoblastic leukemia. *N. Engl. J. Med.* 378: 439–448.
9. Schuster, S. J., M. R. Bishop, C. S. Tam, E. K. Waller, P. Borchmann, J. P. McGuirk, U. Jäger, S. Jaglowski, C. Andreadis, J. R. Westin, et al; JULIET Investigators. 2019. Tisagenlecleucel in adult relapsed or refractory diffuse large B-cell lymphoma. *N. Engl. J. Med.* 380: 45–56.
10. Locke, F. L., S. S. Neelapu, N. L. Bartlett, T. Siddiqi, J. C. Chavez, C. M. Hosing, A. Ghobadi, L. E. Budde, A. Bot, J. M. Rossi, et al. 2017. Phase 1 results of ZUMA-1: a multicenter study of KTE-C19 anti-CD19 CAR T cell therapy in refractory aggressive lymphoma. *Mol. Ther.* 25: 285–295.
11. Park, J. H., I. Rivière, M. Gonen, X. Wang, B. Sénéchal, K. J. Curran, C. Sauter, Y. Wang, B. Santomasso, E. Mead, et al. 2018. Long-Term follow-up of CD19 CAR therapy in acute lymphoblastic leukemia. *N. Engl. J. Med.* 378: 449–459.
12. Gardner, R. A., O. Finney, C. Annesley, H. Brakke, C. Summers, K. Leger, M. Bleakley, C. Brown, S. Mgebroff, K. S. Kelly-Spratt, et al. 2017. Intent-to-treat leukemia remission by CD19 CAR T cells of defined formulation and dose in children and young adults. *Blood* 129: 3322–3331.
13. Xu, X., Q. Sun, X. Liang, Z. Chen, X. Zhang, X. Zhou, M. Li, H. Tu, Y. Liu, S. Tu, and Y. Li. 2019. Mechanisms of relapse after CD19 CAR T-cell therapy for acute lymphoblastic leukemia and its prevention and treatment strategies. *Front. Immunol.* 10: 2664.
14. Beckwith, K. A., J. C. Byrd, and N. Muthusamy. 2015. Tetraspanins as therapeutic targets in hematological malignancy: a concise review. *Front. Physiol.* 6: 91.
15. van Spriel, A. B., S. de Keijzer, A. van der Schaaf, K. H. Gartlan, M. Sofi, A. Light, P. C. Linssen, J. B. Boezeman, M. Zuidscherwoude, I. Reinieren-Beeren, et al. 2012. The tetraspanin CD37 orchestrates the α(4)β(1) integrin-Akt signaling axis and supports long-lived plasma cell survival. *Sci. Signal.* 5: ra82.
16. van Spriel, A. B., K. L. Puls, M. Sofi, D. Pouniotis, H. Hochrein, Z. Orinska, K. P. Knobeloch, M. Plebanski, and M. D. Wright. 2004. A regulatory role for CD37 in T cell proliferation. *Journal of immunology (Baltimore, Md.: 1950)* 172: 2953–2961.
17. Sheng, K. C., A. B. van Spriel, K. H. Gartlan, M. Sofi, V. Apostolopoulos, L. Ashman, and M. D. Wright. 2009. Tetraspanins CD37 and CD151 differentially regulate Ag presentation and T-cell co-stimulation by DC. *Eur. J. Immunol.* 39: 50–55.
18. Lapalombella, R., Y. Y. Yeh, L. Wang, A. Ramanunni, S. Rafiq, S. Jha, J. Staubli, D. M. Lucas, R. Mani, S. E. Herman, et al. 2012. Tetraspanin CD37 directly mediates transduction of survival and apoptotic signals. *Cancer Cell* 21: 694–708.
19. Schwartz-Albiez, R., B. Dorken, W. Hofmann, and G. Moldenhauer. 1988. The B cell-associated CD37 antigen (gp40-52). Structure and subcellular expression of an extensively glycosylated glycoprotein. *Journal of immunology (Baltimore, Md.: 1950)* 140: 905–914.
20. van Spriel, A. B., M. Sofi, K. H. Gartlan, A. van der Schaaf, I. Verschueren, R. Torensma, R. A. Raymakers, B. E. Loveland, M. G. Netea, G. J. Adema, et al. 2009. The tetraspanin protein CD37 regulates IgA responses and anti-fungal immunity. *PLoS Pathog.* 5: e1000338.
21. Barrena, S., J. Almeida, M. Yunta, A. López, N. Fernández-Mosteirín, M. Giralt, M. Romero, L. Perdiguer, M. Delgado, A. Orfao, and P. A. Lazo. 2005. Aberrant expression of tetraspanin molecules in B-cell chronic lymphoproliferative disorders and its correlation with normal B-cell maturation. *Leukemia* 19: 1376–1383.
22. Moore, K., S. A. Cooper, and D. B. Jones. 1987. Use of the monoclonal antibody WR17, identifying the CD37 gp40-45 Kd antigen complex, in the diagnosis of B-lymphoid malignancy. *J. Pathol.* 152: 13–21.
23. Gaudio, E., C. Tarantelli, A. Arribas, L. Cascione, I. Kwee, A. Rinaldi, M. Ponzoni, R. Pittau Bordone, G. Stussi, D. Rossi, et al. 2016. Identification of anti-lymphoma biomarkers of response to the anti-CD37 antibody drug conjugate (ADC) IMGN529. *Blood* 128: 4187.
24. Pereira, D. S., C. I. Guevara, L. Jin, N. Mbong, A. Verlinsky, S. J. Hsu, H. Aviña, S. Karki, J. D. Abad, P. Yang, et al. 2015. AGS67E, an anti-CD37 monomethyl auristatin E antibody-drug conjugate as a potential therapeutic for B/T-cell malignancies and AML: a new role for CD37 in AML. *Mol. Cancer Ther.* 14: 1650–1660.
25. Heider, K. H., K. Kiefer, T. Zenz, M. Volden, S. Stilgenbauer, E. Ostermann, A. Baum, H. Lamche, Z. Küpcü, A. Jacobi, et al. 2011. A novel Fc-engineered monoclonal antibody to CD37 with enhanced ADCC and high proapoptotic activity for treatment of B-cell malignancies. *Blood* 118: 4159–4168.
26. Zhao, X., R. Lapalombella, T. Joshi, C. Cheney, A. Gowda, M. S. Hayden-Ledbetter, P. R. Baum, T. S. Lin, D. Jarjoura, A. Lehman, et al. 2007. Targeting CD37-positive lymphoid malignancies with a novel engineered small modular immunopharmaceutical. *Blood* 110: 2569–2577.
27. Hill, J. A., S. Giralt, T. R. Torgerson, and H. M. Lazarus. 2019. CAR-T - and a side order of IgG, to go? - immunoglobulin replacement in patients receiving CAR-T cell therapy. *Blood Rev.* 38: 100596.
28. Kochenderfer, J. N., M. E. Dudley, S. A. Feldman, W. H. Wilson, D. E. Spaner, I. Maric, M. Stetler-Stevenson, G. Q. Phan, M. S. Hughes, R. M. Sherry, et al. 2012. B-cell depletion and remissions of malignancy along with cytokine-associated toxicity in a clinical trial of anti-CD19 chimeric-antigen-receptor-transduced T cells. *Blood* 119: 2709–2720.
29. Brentjens, R. J., I. Rivière, J. H. Park, M. L. Davila, X. Wang, J. Stefanski, C. Taylor, R. Yeh, S. Bartido, O. Borquez-Ojeda, et al. 2011. Safety and persistence of adoptively transferred autologous CD19-targeted T cells in patients with relapsed or chemotherapy refractory B-cell leukemias. *Blood* 118: 4817–4828.
30. Alcantara, M., M. Tesio, C. H. June, and R. Houot. 2018. CAR T-cells for T-cell malignancies: challenges in distinguishing between therapeutic, normal, and neoplastic T-cells. *Leukemia* 32: 2307–2315.
31. Ying, Z., X. F. Huang, X. Xiang, Y. Liu, X. Kang, Y. Song, X. Guo, H. Liu, N. Ding, T. Zhang, et al. 2019. A safe and potent anti-CD19 CAR T cell therapy. *Nat. Med.* 25: 947–953.
32. Hudecek, M., D. Sommermeyer, P. L. Kosasih, A. Silva-Benedict, L. Liu, C. Rader, M. C. Jensen, and S. R. Riddell. 2015. The nonsignaling extracellular spacer domain of chimeric antigen receptors is decisive for in vivo antitumor activity. *Cancer Immunol. Res.* 3: 125–135.
33. Guest, R. D., R. E. Hawkins, N. Kirillova, E. J. Cheadle, J. Arnold, A. O'Neill, J. Irlam, K. A. Chester, J. T. Kemshead, D. M. Shaw, et al. 2005. The role of extracellular spacer regions in the optimal design of chimeric immune receptors: evaluation of four different scFvs and antigens. *Journal of immunotherapy (Hagerstown, Md.: 1997)* 28: 203–211.
34. Fitzer-Attas, C. J., D. G. Schindler, T. Waks, and Z. Eshhar. 1998. Harnessing Syk family tyrosine kinases as signaling domains for chimeric single chain of the variable domain receptors: optimal design for T cell activation. *Journal of immunology (Baltimore, Md.: 1950)* 160: 145–154.
35. Scarfò, I., M. Ormhøj, M. J. Frigault, A. P. Castano, S. Lorrey, A. A. Bouffard, A. van Scoyk, S. J. Rodig, A. J. Shay, J. C. Aster, et al. 2018. Anti-CD37 chimeric antigen receptor T cells are active against B- and T-cell lymphomas. [Published erratum appears in 2018 *Blood* 132: 2527.] *Blood* 132: 1495–1506.
36. Köksal, H., P. Dillard, S. E. Josefsson, S. M. Maggadottir, S. Pollmann, A. Fåne, Y. N. Blaker, K. Beiske, K. Huse, A. Kolstad, et al. 2019. Preclinical

development of CD37CAR T-cell therapy for treatment of B-cell lymphoma. *Blood Adv.* 3: 1230–1243.
37. Watanabe, K., S. Terakura, A. C. Martens, T. van Meerten, S. Uchiyama, M. Imai, R. Sakemura, T. Goto, R. Hanajiri, N. Imahashi, et al. 2015. Target antigen density governs the efficacy of anti-CD20-CD28-CD3 ζ chimeric antigen receptor-modified effector CD8+ T cells. *J. Immunol.* 194: 911–920.
38. Lenkei, R., J. W. Gratama, G. Rothe, G. Schmitz, J. L. D'hautcourt, A. Arekrans, F. Mandy, and G. Marti. 1998. Performance of calibration standards for antigen quantitation with flow cytometry. *Cytometry* 33: 188–196.
39. Wang, X., W. C. Chang, C. W. Wong, D. Colcher, M. Sherman, J. R. Ostberg, S. J. Forman, S. R. Riddell, and M. C. Jensen. 2011. A transgene-encoded cell surface polypeptide for selection, in vivo tracking, and ablation of engineered cells. *Blood* 118: 1255–1263.
40. Sakemura, R., S. Terakura, K. Watanabe, J. Julamanee, E. Takagi, K. Miyao, D. Koyama, T. Goto, R. Hanajiri, T. Nishida, et al. 2016. A tet-on inducible system for controlling CD19-chimeric antigen receptor expression upon drug administration. *Cancer Immunol. Res.* 4: 658–668.
41. Gonzalez, L., N. Strbo, and E. R. Podack. 2013. Humanized mice: novel model for studying mechanisms of human immune-based therapies. *Immunol. Res.* 57: 326–334.
42. de Winde, C. M., M. Zuidscherwoude, A. Vasaturo, A. van der Schaaf, C. G. Figdor, and A. B. van Spriel. 2015. Multispectral imaging reveals the tissue distribution of tetraspanins in human lymphoid organs. *Histochem. Cell Biol.* 144: 133–146.
43. Wood, B. 2004. Multicolor immunophenotyping: human immune system hematopoiesis. *Methods Cell Biol.* 75: 559–576.
44. Richman, S. A., S. Nunez-Cruz, B. Moghimi, L. Z. Li, Z. T. Gershenson, Z. Mourelatos, D. M. Barrett, S. A. Grupp, and M. C. Milone. 2018. High-affinity GD2-specific CAR T cells induce fatal encephalitis in a preclinical neuroblastoma model. *Cancer Immunol. Res.* 6: 36–46.
45. Qian, L., D. Li, L. Ma, T. He, F. Qi, J. Shen, and X. A. Lu. 2016. The novel anti-CD19 chimeric antigen receptors with humanized scFv (single-chain variable fragment) trigger leukemia cell killing. *Cell. Immunol.* 304–305: 49–54.
46. Hudecek, M., M. T. Lupo-Stanghellini, P. L. Kosasih, D. Sommermeyer, M. C. Jensen, C. Rader, and S. R. Riddell. 2013. Receptor affinity and extracellular domain modifications affect tumor recognition by ROR1-specific chimeric antigen receptor T cells. *Clin. Cancer Res.* 19: 3153–3164.
47. Hosen, N., Y. Matsunaga, K. Hasegawa, H. Matsuno, Y. Nakamura, M. Makita, K. Watanabe, M. Yoshida, K. Satoh, S. Morimoto, et al. 2017. The activated conformation of integrin $\beta_7$ is a novel multiple myeloma-specific target for CAR T cell therapy. *Nat. Med.* 23: 1436–1443.
48. Imai, C., K. Mihara, M. Andreansky, I. C. Nicholson, C. H. Pui, T. L. Geiger, and D. Campana. 2004. Chimeric receptors with 4-1BB signaling capacity provoke potent cytotoxicity against acute lymphoblastic leukemia. *Leukemia* 18: 676–684.
49. Carpenito, C., M. C. Milone, R. Hassan, J. C. Simonet, M. Lakhal, M. M. Suhoski, A. Varela-Rohena, K. M. Haines, D. F. Heitjan, S. M. Albelda, et al. 2009. Control of large, established tumor xenografts with genetically retargeted human T cells containing CD28 and CD137 domains. *Proc. Natl. Acad. Sci. USA* 106: 3360–3365.
50. Zhao, Z., M. Condomines, S. J. C. van der Stegen, F. Perna, C. C. Kloss, G. Gunset, J. Plotkin, and M. Sadelain. 2015. Structural design of engineered costimulation determines tumor rejection kinetics and persistence of CAR T cells. *Cancer Cell* 28: 415–428.
51. Cooper, M. L., J. Choi, K. Staser, J. K. Ritchey, J. M. Devenport, K. Eckardt, M. P. Rettig, B. Wang, L. G. Eissenberg, A. Ghobadi, et al. 2018. An "off-the-shelf" fratricide-resistant CAR-T for the treatment of T cell hematologic malignancies. *Leukemia* 32: 1970–1983.
52. Gomes-Silva, D., E. Atilla, P. A. Atilla, F. Mo, H. Tashiro, M. Srinivasan, P. Lulla, R. H. Rouce, J. M. S. Cabral, C. A. Ramos, et al. 2019. CD7 CAR T cells for the therapy of acute myeloid leukemia. *Mol. Ther.* 27: 272–280.
53. Xiong, W., Y. Chen, X. Kang, Z. Chen, P. Zheng, Y. H. Hsu, J. H. Jang, L. Qin, H. Liu, G. Dotti, and D. Liu. 2018. Immunological synapse predicts effectiveness of chimeric antigen receptor cells. [Published erratum appears in 2021 *Mol Ther.* 29: 1349–1351.] *Mol. Ther.* 26: 963–975.
54. Schwartz-Albiez, R., B. Dörken, W. Hofmann, and G. Moldenhauer. 1988. The B cell-associated CD37 antigen (gp40-52). Structure and subcellular expression of an extensively glycosylated glycoprotein. *J. Immunol.* 140: 905–914.